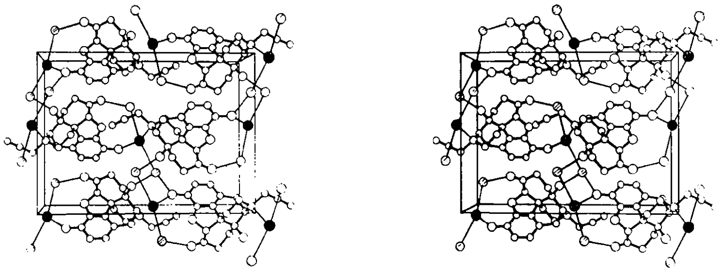

Fig. 4. Packing of naloxone.HCl.$2H_2O$. The solid circles represent the Cl^- ions while the shaded circles represent the O atoms in the H_2O molecules. The directions of the axes are $a\downarrow$, $b\rightarrow$ and c directed toward the viewer.

potent than the corresponding agonist oxymorphone (Pert, Pasternak & Snyder, 1973) where the only chemical difference in the molecules is the substitution of an allyl side chain for the methyl group on the N atom.

The substitution of CH_2-◁ for $CH_2CH=CH_2$ in naloxone yields compound EN-1639 in which some of the favorable properties of naloxone are increased. The conformation of EN-1639 can be predicted by combining the conformational parameters of naloxone with those of the N-CH-◁ moiety in cyclazocine (see the previous section).

This project was supported in part by the Office of Naval Research, Project Order P04-0095.

References

ALTONA, C., GEISE, H. J. & ROMERS, C. (1968). *Tetrahedron*, pp. 13–32.

BÜRGI, H. B., DUNITZ, J. D. & SHEFTER, E. (1973). *Nature New Biol.* **244**, 186–187.

Chem. Eng. News (1972). 2 July, pp. 14–15.

EDDY, N. B. & MAY, E. L. (1973). *Science*, **181**, 407–414.

GYLBERT, L. (1973). *Acta Cryst.* B**29**, 1630–1635.

KARLE, I. L., GILARDI, R. D., FRATINI, A. V. & KARLE, J. (1969). *Acta Cryst.* B**25**, 1469–1479.

KARLE, J. & KARLE, I. L. (1966). *Acta Cryst.* **21**, 849–859.

KARTHA, G., AHMED, F. R. & BARNES, W. H. (1962). *Acta Cryst.* **15**, 326–333.

KOROLKOVAS, A. (1970). *Essentials of Molecular Pharmacology, Background for Drug Design*, p. 123. New York: John Wiley.

LINDSEY, J. M. & BARNES, W. H. (1955). *Acta Cryst.* **8**, 227–232.

MACKAY, M. & HODGKIN, D. C. (1955). *J. Chem. Soc.* pp. 3261–3267.

PERT, C. B., PASTERNAK, G. & SNYDER, S. H. (1973). *Science*, **182**, 1359–1361.

PERT, C. B. & SNYDER, S. H. (1973). *Science*, **179**, 1011–1014.

Acta Cryst. (1974). B**30**, 1686

The Crystal and Molecular Structure of Hexakis(pyridine-*N*-oxide)nickel(II) Bis(tetrafluoroborate)

BY A. D. VAN INGEN SCHENAU, G. C. VERSCHOOR AND C. ROMERS

Chemical Department, X-ray and Electron Diffraction Section, University of Leiden, P.O. Box 75, Leiden, The Netherlands

(*Received* 11 *February* 1974; *accepted* 7 *March* 1974)

Crystals of $Ni(PyNO)_6(BF_4)_2$ are rhombohedral, with $a=12{\cdot}487$ (5) and $c=18{\cdot}92$ (1) Å for the hexagonal cell (rhombohedral cell: $a=9{\cdot}579$ Å, $\alpha=81{\cdot}36°$); $Z=3$. Diffractometer data (Mo $K\alpha$ radiation) were collected up to $\theta=35°$. Anisotropic refinement was carried out with 2163 observed independent reflexions. Two models were refined, one in space group $R3$, the other in $R\bar{3}$. The final R_w values are 0·037 and 0·046 for space groups $R3$ and $R\bar{3}$ respectively. Both models contain disordered BF_4 groups. The ambiguity in choice of space group is discussed. Atomic parameters of both models are given. Geometrical data are based on the centrosymmetric model. The coordination of the Ni cation is nearly octahedral. Each $Ni(PyNO)_6$ group is surrounded by eight tetrafluoroborate groups. Lattice dimensions of a number of isomorphous complexes are presented.

Introduction

Complexes M(II) $(PyNO)_6(\text{Anion})_2$ (PyNO = pyridine-*N*-oxide) of metals of the first transition series with the anions BF_4^- and ClO_4^- have been investigated by several authors. Reviews on the coordination chemistry of aromatic *N*-oxide compounds have been given by Garvey, Nelson & Ragsdale (1968) and Karayannis, Pytlewski & Mikulski (1973). At our laboratory the preparation and the infrared, far-infrared, UVV, e.p.r. and Mössbauer spectra of these compounds have been investigated by Reedijk (1969).

Detailed knowledge of the crystal structure of at least one of these compounds is necessary for the interpretation of the far-infrared spectra, which were studied by van Ingen Schenau, Reedijk & Groeneveld (1974). $Ni(PyNO)_6(BF_4)_2$ was chosen for this single-crystal study.

The results of the structure determination will be compared with earlier conclusions from different physical measurements. In addition a comparison is made between the structure of this compound and the recently published structure of $Hg(PyNO)_6(ClO_4)_2$ (Kepert, Taylor & White, 1973).

The isomorphism of the compounds $M(II)\,(PyNO)_6(ClO_4)_2$ and $M(II)\,(PyNO)_6(BF_4)_2$ with M = Mn, Fe, Co, Ni, Cu, Zn, Hg and Mg is established by means of powder diffraction diagrams.

A forthcoming paper will deal with the vibrational analysis of the compound based on X-ray data and far-infrared spectra.

Experimental

Preparation

The complex was obtained by blending alcoholic solutions of pyridine-*N*-oxide and the hydrated $Ni(BF_4)_2$ salt, as described by Kakiuti, Kida & Quagliano (1963). Crystals were grown by very slow evaporation of a saturated alcoholic solution of the complex at room temperature. A small amount of triethyl orthoformate was added as dehydrating agent (van Leeuwen & Groeneveld, 1967). Melting point, metal analysis and infrared and UVV spectra were in accordance with literature data (Reedijk, 1969; Pappas, Osterman & Powell, 1970).

Powder diagrams

X-ray powder diffraction data (Cu $K\alpha_1$, $\lambda = 1·5405$) were collected for compounds with the general formula $M^{II}(PyNO)_6(Anion)_2$, with the anions tetrafluoroborate and perchlorate; M = Mg, Mn, Fe, Co, Ni, Cu, Zn and Hg. Approximate cell constants (±0·03 Å) were calculated from 15 low-angle reflexions, which we could assign unambiguously. Difficulties occurred in the assignment of lines at Bragg angles above 30°, owing to the coincidence of many reflexions. Table 1 gives the cell constants, calculated by least-squares refinement of estimates for *a*, *c* and zero-point correction. The isomorphism of these compounds is in agreement with far-infrared data (van Ingen Schenau, Reedijk & Groeneveld, 1974). The compound $Cd(PyNO)_6(ClO_4)_2$ is probably of another type.

Table 1. *Approximate cell constants of isomorphous* $M^{II}(PyNO)_6(Anion)_2$ *compounds*

Compound	*a*	*c*	Unit-cell volume
$Mn(PyNO)_6(BF_4)_2$	12·66	19·21	2665
$Co(PyNO)_6(BF_4)_2$	12·55	18·96	2584
$Ni(PyNO)_6(BF_4)_2$	12·51	18·95	2570
$Cu(PyNO)_6(BF_4)_2$	12·54	18·92	2574
$Zn(PyNO)_6(BF_4)_2$	12·55	19·01	2592
$Mg(PyNO)_6(ClO_4)_2$	12·58	19·05	2612
$Mn(PyNO)_6(ClO_4)_2$	12·60	19·20	2638
$Fe(PyNO)_6(ClO_4)_2$	12·60	19·17	2635
$Co(PyNO)_6(ClO_4)_2$	12·53	19·06	2592
$Ni(PyNO)_6(ClO_4)_2$	12·48	19·04	2567
$Cu(PyNO)_6(ClO_4)_2$	12·53	19·09	2594
$Zn(PyNO)_6(ClO_4)_2$	12·52	19·11	2596
$Hg(PyNO)_6(ClO_4)_2$	12·68	19·35	2693

Collection and reduction of diffraction data

Preliminary Weissenberg investigations showed the Laue group to be $\bar{3}$. Cell constants were accurately measured on a diffractometer, using Ni-filtered Cu $K\alpha$ radiation ($\lambda = 1·5418$ Å). An approximately rectangular crystal with edges of 0·3, 0·4 and 0·5 mm was selected for the intensity measurements. The faces of the crystal corresponded to (100), (010) and (001) of the rhombohedral cell. The reflexion intensities were

Table 2. *Technical and crystal data of* $Ni(PyNO)_6(BF_4)_2$

Estimated standard deviations in the least significant digits are given in parentheses for this and following tables.

Space group	$R3$ or $R\bar{3}$	Hexagonal description
a	9·579 (3) Å	12·487 (5) Å
c		18·920 (10) Å
α	81·36 (3)°	
V	851·7 Å^3	2555·0 Å^3
Z	1	3
M.W.	802·67	
d(calc.)	1·564 g cm^{-3}	
λ(Mo $K\alpha$)	0·71069 Å	
μ(Mo $K\alpha$)	4·3 cm^{-1}	
Bragg angle	0°–35°	
Scan type	ω	
Scan angle	$1·3° + 0·9 \tan\theta$	
Scan time	± 120 s/reflexion + background	
Monochromator	graphite	
Measured reflexions	4700	
Independent reflexions (significant)	2163	
Independent reflexions (not significant)	415	

recorded with an Enraf–Nonius three-circle single-crystal diffractometer, using graphite monochromatized Mo $K\alpha$ radiation ($\lambda=0{\cdot}71069$ Å). The crystal was mounted with the plane (508) perpendicular to the φ axis of the instrument. Crystal data and technical information are given in Table 2.

A lower limit of twice the standard deviation $\sigma(I)$ of the intensity measurements was adopted for the observed reflexions. The values of these σ's were calculated from the statistical inaccuracy of the measurements, taking into account errors in the absorption correction and attenuation filters.

A correction was made for absorption effects, with a Fortran IV program developed by de Graaff (1973). Calculated transmission factors are between 0·80 and 0·85. After correction for Lorentz and polarization effects the intensities were reduced to F_o values and the symmetry-related reflexions were averaged. A Wilson plot was calculated in order to obtain approximate values for the scale factor and the overall isotropic thermal parameter B.

Structure determination

Scattering factors for nickel were taken from Cromer & Waber (1965) and for the light atoms from *International Tables for X-ray Crystallography* (1962). The scattering of Ni(II) was corrected for the real part of the anomalous dispersion of Mo $K\alpha$ radiation. The imaginary part was not taken into account.

An electron distribution of 9·5 e for fluorine and 4 e for boron was assumed for the description of the scattering of the BF_4^- anions, in order to account for the covalent bonding in tetrafluoroborate. Scattering factors for $F^{1/2-}$ were calculated by averaging the values of F^- and F^0.

The structure was solved by direct methods, in particular by means of the multisolution method (Germain & Woolfson, 1968; Karle, 1968). Normalized structure factors E were calculated. The Wilson statistics $\langle|E|\rangle=0{\cdot}871$ and $\langle|E^2-1|\rangle=0{\cdot}760$ (Table 4) point to the non-centrosymmetric space group. Two hundred strong reflexions ($E>1{\cdot}58$) were selected, giving 8206 non-redundant $\sum_2$ relations. The reflexion $53\overline{1}$ ($E=2{\cdot}19$) was selected as origin-defining (Gramaccioli & Zechmeister, 1972). Trial phases $-\frac{3}{4}\pi$, $-\frac{1}{4}\pi$, $\frac{1}{4}\pi$ and $\frac{3}{4}\pi$ were assigned to the reflexions 8,0,14 ($E=3{\cdot}01$) and $5\overline{2}7$ ($E=2{\cdot}58$) and phases $-\frac{3}{4}\pi$ and $-\frac{1}{4}\pi$ were assigned to the reflexion $\overline{3}$,7,14 ($E=2{\cdot}52$), thereby fixing the enantiomorph. Table 3 gives the final results of nine solutions with a low value for R_{Karle}. A number of trivial solutions appeared, with very low R_{Karle} and a high consistency. Similar effects have been reported by Schenk (1972).

To avoid this type of solution an additional acceptance criterion was added to the program. The multisolution program produced 32 sets of phases with φ's ranging from $-\pi$ to $+\pi$. For each solution values for $|\langle\varphi\rangle|$ and $\langle|\varphi|\rangle$ were calculated. For centrosymmetric as well as non-centrosymmetric structures with a large number of atoms in the asymmetric unit, values for $|\langle\varphi\rangle|$ and $\langle|\varphi|\rangle$ should approach 0 and $\frac{1}{2}\pi$ respectively. For a trivial or 'Patterson' solution the values for $|\langle\varphi\rangle|$ and $\langle|\varphi|\rangle$ are nearly equal.

Table 3. *Comparison of results of the multisolution program*

No.	Starting set reflexions 8,0,14	$5\overline{2}7$	$\overline{3}$,7,14	R_{Karle}	t	α	$\langle\varphi\rangle$	$\langle\lvert\varphi\rvert\rangle$
1	$-\frac{3}{4}\pi$	$-\frac{3}{4}\pi$	$-\frac{3}{4}\pi$	10	0·98	288	$0{\cdot}178\pi$	$0{\cdot}178\pi$
2	$-\frac{3}{4}\pi$	$-\frac{1}{4}\pi$	$-\frac{3}{4}\pi$	10	0·99	291	$0{\cdot}116\pi$	$0{\cdot}116\pi$
3	$-\frac{3}{4}\pi$	$\frac{1}{4}\pi$	$-\frac{3}{4}\pi$	15	0·73	213	$-0{\cdot}034\pi$	$0{\cdot}470\pi$
4	$-\frac{3}{4}\pi$	$\frac{3}{4}\pi$	$-\frac{3}{4}\pi$	10	0·97	283	$0{\cdot}258\pi$	$0{\cdot}260\pi$
5	$-\frac{1}{4}\pi$	$-\frac{3}{4}\pi$	$-\frac{3}{4}\pi$	10	0·95	277	$0{\cdot}330\pi$	$0{\cdot}330\pi$
6	$-\frac{1}{4}\pi$	$-\frac{3}{4}\pi$	$-\frac{1}{4}\pi$	12	0·84	247	$0{\cdot}194\pi$	$0{\cdot}550\pi$
7	$-\frac{1}{4}\pi$	$-\frac{1}{4}\pi$	$-\frac{1}{4}\pi$	11	0·87	254	$0{\cdot}314\pi$	$0{\cdot}524\pi$
8	$-\frac{1}{4}\pi$	$\frac{1}{4}\pi$	$-\frac{1}{4}\pi$	15	0·75	220	$0{\cdot}054\pi$	$0{\cdot}508\pi$
9	$-\frac{1}{4}\pi$	$\frac{3}{4}\pi$	$-\frac{1}{4}\pi$	15	0·72	221	$-0{\cdot}042\pi$	$0{\cdot}480\pi$

$$R_{\text{Karle}}=\frac{\sum\big||E_{\mathbf{h}}|-|E_{\mathbf{h}\,\text{calc}}|\big|}{\sum|E_{\mathbf{h}}|}\;;A=\sum_{\mathbf{k}}|E_{\mathbf{k}}|\,.\,|E_{\mathbf{h}-\mathbf{k}}|\cos(\varphi_{\mathbf{k}}+\varphi_{\mathbf{h}-\mathbf{k}})$$

$$t=\frac{(A^2+B^2)^{1/2}}{\sum_{\mathbf{k}}|E_{\mathbf{k}}|-|E_{\mathbf{h}-\mathbf{k}}|}\;;B=\sum_{\mathbf{k}}|E_{\mathbf{k}}|\,.\,|E_{\mathbf{h}-\mathbf{k}}|\sin(\varphi_{\mathbf{k}}+\varphi_{\mathbf{h}-\mathbf{k}})$$

$$\alpha=|E_{\mathbf{h}}|(A^2+B^2)^{1/2}$$

We used the values for $|\langle\varphi\rangle|$ and $\langle|\varphi|\rangle$ as an indication that the starting sets 3, 8 and 9 of Table 3 were more reliable than the rest. An E map based on the phases of solution 8 contained two images of the structure related by a centre of symmetry. Solutions 3 and 9 were similar but were shifted with respect to the pseudo-origin.

Least-squares refinement was started at this stage with a non-centrosymmetric model. The function minimized during the refinement process was: $\sum w(|F_o|-|F_c|)^2$ with the weighting scheme $w=\sigma_{F_o}^{-2}$. The discrepancy indices are defined as $R=\sum||F_o|-|F_c||/\sum|F_o|$ and $R_w=[\sum w(|F_o|-|F_c|)^2/\sum w|F_o|^2]^{1/2}$. The refinement was performed with 2163 statistically significant independent reflexions. The Ni atom was placed at $0,0,\frac{1}{2}$ and the ring and anion atoms at positions deduced from one enantiomorph of the E map. The full-matrix isotropic refinement rapidly converged to $R_w=0{\cdot}12$. After this stage several difficulties arose. First, the model refined to a nearly centrosymmetric structure. The second problem was the position of the BF_4^- groups. We decided to perform two refinements: one with a centrosymmetric model, space group $R\overline{3}$, with disordered BF_4^- groups, the other with a non-centrosymmetric model in space group $R3$, also with disordered anions. The refinements were extended

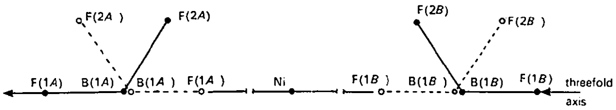

Fig. 1. Arrangement and atomic numbering of the disordered BF_4^- groups in the non-centrosymmetric model.

to anisotropic thermal parameters for the heavy atoms, and hydrogen atoms were placed at positions deduced from a difference Fourier map.

Refinement of the centrosymmetric model

The refinement of the centrosymmetric model was carried out by a full-matrix least-squares minimization. Careful inspection of a difference map as well as Fourier maps based on phase calculations without anion contributions indicated that rotational disorder like that found in triphenylmethyl perchlorate (Gomes de Mesquita, 1962) could be ruled out. Obviously there are two possible orientations for the BF_4^- anion: one with the fluorine atom on the threefold axis directed towards the nickel cation and the other with the corresponding atom pointing to the other side. (Fig. 1). This kind of anion disordering has been found previously in tris-octamethylpyrophosphoramide complexes of Co^{II}, Mg^{II} and Cu^{II} perchlorates (Joesten, Hussain & Lenhert, 1970).

The refinement was started again with this disordered BF_4^- group and one parameter was refined for the relative occupation numbers of both groups. The refinement with 117 parameters and 2163 observed reflexions converged rapidly and finally resulted in $R=0{\cdot}0485$ and $R_w=0{\cdot}0463$.

Final shifts of the parameters were always $<2\%$ of the estimated standard deviation and in most cases $<0{\cdot}1\%$. A final difference Fourier map revealed peaks of about 0·6 e Å^{-3} in the vicinity of Ni. The statistical height of the map was 0·1 e Å^{-3}. A few other peaks, of about 0·3 e Å^{-3}, were positioned between the adjacent ring atoms.

Non-centrosymmetric refinement

In the non-centrosymmetric model we introduced the same disordered BF_4^- groups. On both sides of the nickel atom one parameter was inserted for the refinement of the occupancy ratio of two related BF_4^- groups. The number of parameters was too large for a full-matrix refinement. Because of the very large covariances of the parameters related by the pseudo-symmetry centre, we decided to carry out a block-matrix refinement. The matrix consisted of four blocks, in which all important off-diagonal elements are saved. Block 1: Ni, O(*A*), O(*B*), N(*A*), N(*B*). Block 2: all carbon atoms. Block 3: all anion atoms. Block 4: all hydrogen atoms. Owing to the very high covariances the refinement converged slowly. Final values of the discrepancy indices are $R=0{\cdot}0419$ and $R_w=0{\cdot}0369$ for the

Table 4. *Numerical data for R-ratio tests*

Symbols are explained by Hamilton (1964).

	Non-centrosymmetric model	Centrosymmetric model	Ratio
R_w	0·0369	0·0463	1·255
R	0·0419	0·0485	1·158
n	2163	2163	
p	230	117	$R_{113,\,1933,\,0.005}=1{\cdot}044$

Values for $\langle\lvert E\rvert\rangle$ and $\langle\lvert E^2-1\rvert\rangle$*

	$\langle\lvert E\rvert\rangle$	$\langle\lvert E^2-1\rvert\rangle$
Centrosymmetric model theoretical	0·798	0·968
Non-centrosymmetric model theoretical	0·886	0·736
E_{obs}	0·871	0·760
E_{calc}, centrosymmetric model	0·860	0·787
E_{calc}, $\sin\theta>0{\cdot}25$, centrosymmetric model	0·860	0·784

* Theoretical values of Karle & Hauptman (1956).

Table 5. *Observed and calculated structure factors* (× 10) *on an absolute scale*

Calculated structure factors are based on the non-centrosymmetric model.

Table 5 (*cont.*)

set of 2163 data and 230 parameters. Final parameter shifts were about $\frac{1}{5}$ of the standard deviation. Maximum shifts were about one-half the standard deviation. The final difference Fourier map showed a maximum density of 0·9 e Å^{-3} at the Ni position. The statistical height was 0·1 e Å^{-3}. A few other small peaks were found near the nickel atom, all being smaller than 0·3 e Å^{-3}. The arrangement of peaks in the vicinity of Ni is such that correction with temperature parameters or a different number of electrons for the ion would not be successful. Insufficient accuracy in the scattering factors to describe the actual electron distribution may be responsible for these observed deviations.

Results

We arrive at the unusual conclusion that the statistics favour a non-centrosymmetric distribution, even when based upon calculated structure factors including non-significant reflexions for the centrosymmetric model (Table 4). It may be that the statistical theory only allows for distinctly centrosymmetric or non-centrosymmetric distributions.

A similar conclusion can be drawn from the results of the two refinements. The Hamilton test clearly favours the non-centrosymmetric model, while chemical intuition favours the centrosymmetric structure. A nearly centrosymmetric structure contains atoms at positions x, y, z and $\bar{x}+\xi$, $\bar{y}+\eta$ and $\bar{z}+\sigma$, where ξ, η and σ denote very small deviations. The least-squares procedure has no proper facilities to tackle the problems of small displacements. One might say that both refinements are biased in the sense that the real structure is somewhere in between. Such a result does not indeed contradict the spectroscopic data, since a very small deviation from the centrosymmetric structure cannot be detected.

The observed structure factors and the F_c values of the non-centrosymmetric model are listed in Table 5. Positional and vibrational parameters are given in Tables 6, 7, 8 and 9.

Table 6. *Atomic parameters of the heavy atoms* (*in fractions of cell edges* × 10^4) *of both models*

Estimated standard deviations in the least significant digits are given in parentheses.

Centrosymmetric model

	x/a	y/b	z/c
*Ni	0	0	5000
O	1052 (1)	1522 (1)	4375 (1)
N	492 (1)	2010 (1)	4005 (1)
C(1)	30 (2)	2636 (2)	4331 (1)
C(2)	−530 (2)	3154 (2)	3949 (1)
C(3)	−613 (2)	3024 (2)	3221 (1)
C(4)	−120 (2)	2386 (2)	2904 (1)
C(5)	440 (2)	1882 (2)	3296 (1)
*B	0	0	1478 (3)
*B#	0	0	1490 (7)
*F(1)	0	0	793 (1)
*F(1)#	0	0	2133 (4)
F(2)	−988 (3)	81 (4)	1709 (2)
F(2)#	−961 (14)	39 (17)	1296 (7)

Non-centrosymmetric model

	x/a	y/b	z/c
*Ni	0	0	5000
O(*A*)	1063 (3)	1541 (3)	4370 (2)
N(*A*)	495 (5)	2012 (4)	4012 (2)
C(1*A*)	32 (6)	2619 (6)	4346 (3)
C(2*A*)	−581 (7)	3149 (8)	3962 (3)
C(3*A*)	−607 (7)	3023 (6)	3262 (3)
C(4*A*)	−157 (6)	2425 (6)	2930 (3)
C(5*A*)	445 (6)	1901 (5)	3292 (2)
O(*B*)	−1040 (3)	−1504 (3)	5620 (2)
N(*B*)	−490 (4)	−2005 (3)	6003 (2)
C(1*B*)	−14 (7)	−2658 (6)	5694 (3)
C(2*B*)	482 (7)	−3155 (6)	6060 (4)
C(3*B*)	622 (6)	−3024 (7)	6808 (3)
C(4*B*)	68 (8)	−2338 (6)	7129 (3)
C(5*B*)	−438 (6)	−1870 (5)	6700 (2)
*B(1*A*)	0	0	1485 (7)
*B(1*A*#)	0	0	1484 (27)
*F(1*A*)	0	0	770 (4)
*F(1*A*#)	0	0	2179 (7)
F(2*A*)	−1004 (10)	82 (12)	1759 (3)
F(2*A*#)	−1030 (10)	128 (16)	1464 (5)
*B(1*B*)	0	0	8586 (7)
*B(1*B*#)	0	0	8353 (6)
*F(1*B*)	0	0	9179 (7)
*F(1*B*#)	0	0	7963 (17)
F(2*B*)	962 (9)	−85 (9)	8286 (3)
F(2*B*#)	−713 (16)	−665 (18)	9014 (10)

* Special positions.

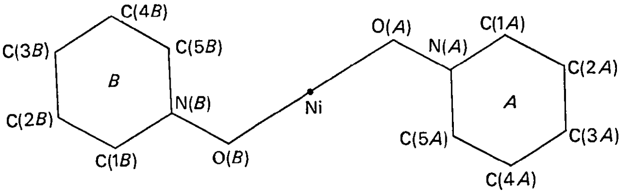

Fig. 2. Atomic numbering of the PyNO molecules in the non-centrosymmetric model.

Table 7. *Atomic coordinates of hydrogen atoms (in fractions of cell edges* $\times 10^3$*) and temperature parameters B* ($Å^2 \times 10$)

Estimated standard deviations in the least significant digits are given in parentheses.

Centrosymmetric model

	x/*a*	*y*/*b*	*z*/*c*	*B* (iso)
H(1)	2 (2)	260 (2)	486 (1)	24 (3)
H(2)	−80 (2)	361 (2)	420 (1)	37 (4)
H(3)	−94 (3)	335 (3)	294 (1)	52 (5)
H(4)	−11 (2)	225 (3)	236 (1)	54 (5)
H(5)	79 (2)	142 (2)	312 (1)	18 (3)

Non-centrosymmetric model

	x/*a*	*y*/*b*	*z*/*c*	*B* (iso)
H(1*A*)	27 (3)	276 (4)	486 (1)	19 (6)
H(2*A*)	−91 (3)	357 (3)	417 (1)	19 (5)
H(3*A*)	−78 (4)	330 (5)	291 (2)	41 (10)
H(4*A*)	20 (4)	245 (4)	231 (2)	39 (9)
H(5*A*)	82 (4)	144 (4)	315 (1)	10 (7)
H(1*B*)	16 (4)	−250 (4)	525 (1)	26 (7)
H(2*B*)	65 (6)	−387 (5)	563 (2)	81 (17)
H(3*B*)	111 (5)	−337 (5)	703 (2)	46 (11)
H(4*B*)	30 (3)	−212 (3)	761 (1)	17 (5)
H(5*B*)	−81 (5)	−153 (5)	693 (1)	27 (10)

Table 8. *Vibrational parameters of cation atoms,* $U(ij) \times 10^3$ ($Å^2$)

Estimated standard deviations in the least significant digits are given in parentheses.

Centrosymmetric model

	U(11)	*U*(22)	*U*(33)	2*U*(12)	2*U*(23)	2*U*(31)
*Ni	35 (0)	35 (0)	27 (0)	35 (0)	0	0
O	39 (0)	43 (0)	41 (0)	43 (1)	20 (0)	7 (0)
N	37 (0)	32 (0)	38 (0)	29 (1)	15 (0)	7 (0)
C(1)	71 (1)	51 (1)	56 (0)	76 (1)	26 (1)	34 (1)
C(2)	75 (1)	60 (1)	96 (1)	92 (2)	50 (2)	46 (2)
C(3)	62 (1)	52 (1)	102 (1)	50 (2)	53 (2)	−30 (2)
C(4)	71 (1)	43 (1)	58 (0)	31 (1)	16 (1)	−41 (1)
C(5)	55 (0)	36 (0)	40 (0)	33 (1)	4 (0)	−4 (1)

Non-centrosymmetric model

	U(11)	*U*(22)	*U*(33)	2*U*(12)	2*U*(23)	2*U*(31)
*Ni	35 (0)	35 (0)	28 (0)	35 (0)	0	0
O(*A*)	46 (2)	47 (2)	38 (1)	54 (3)	30 (2)	4 (2)
N(*A*)	39 (2)	45 (2)	36 (1)	37 (4)	23 (3)	15 (3)
C(1*A*)	75 (3)	59 (3)	50 (1)	105 (6)	35 (4)	25 (4)
C(2*A*)	69 (4)	77 (4)	86 (3)	103 (7)	58 (6)	37 (6)
C(3*A*)	72 (4)	47 (3)	112 (4)	72 (5)	33 (6)	−42 (6)
C(4*A*)	65 (3)	40 (2)	50 (1)	34 (4)	19 (3)	−46 (3)
C(5*A*)	61 (3)	40 (2)	33 (1)	30 (5)	−8 (3)	−2 (4)
O(*B*)	32 (1)	39 (1)	44 (1)	31 (2)	12 (2)	11 (2)
N(*B*)	35 (2)	20 (1)	41 (1)	20 (3)	7 (2)	0 (3)
C(1*B*)	76 (3)	44 (3)	59 (2)	51 (5)	23 (4)	52 (4)
C(2*B*)	74 (4)	49 (3)	106 (4)	86 (6)	49 (6)	54 (6)
C(3*B*)	52 (3)	57 (3)	86 (2)	26 (5)	68 (5)	−30 (4)
C(4*B*)	76 (3)	40 (2)	64 (2)	34 (5)	1 (3)	−21 (4)
C(5*B*)	48 (3)	31 (2)	48 (2)	32 (4)	16 (3)	−7 (4)

* Special positions.

Table 9. *Vibrational parameters of anion atoms,* $U(ij) \times 10^2$ ($Å^2$)

Estimated standard deviations in the least significant digits are given in parentheses.

Centrosymmetric model

	U(11)	*U*(22)	*U*(33)	2*U*(12)	2*U*(23)	2*U*(31)
*B	5 (0)	5 (0)	5 (0)	5 (0)	0	0
*B#	33 (4)	33 (4)	0 (0)	33 (4)	0	0
*F(1)	15 (0)	15 (0)	5 (0)	15 (0)	0	0
*F(1)#	20 (1)	20 (1)	4 (0)	20 (1)	0	0
F(2)	10 (0)	15 (0)	15 (0)	15 (0)	−1 (0)	9 (0)
F(2)#	13 (1)	21 (1)	30 (1)	19 (2)	6 (3)	−23 (2)

Non-centrosymmetric model

	U(11)	*U*(22)	*U*(33)	2*U*(12)	2*U*(23)	2*U*(31)
*B(1*A*)	6 (0)	6 (0)	0 (0)	6 (0)	0	0
*B(1*A*#)	44 (7)	44 (7)	3 (1)	44 (7)	0	0
*F(1*A*)	12 (0)	12 (0)	3 (0)	12 (0)	0	0
*F(1*A*#)	23 (1)	23 (1)	4 (0)	23 (1)	0	0
F(2*A*)	10 (0)	13 (0)	10 (0)	12 (1)	0 (1)	10 (1)
F(2*A*#)	7 (0)	21 (1)	8 (0)	20 (1)	0 (1)	0 (1)
*B(1*B*)	5 (0)	5 (0)	3 (0)	5 (0)	0	0
*B(1*B*#)	5 (0)	5 (0)	−1 (0)	5 (0)	0	0
*F(1*B*)	19 (1)	19 (1)	5 (0)	19 (1)	0	0
*F(1*B*#)	44 (6)	44 (6)	2 (1)	44 (6)	0	0
F(2*B*)	13 (0)	14 (0)	14 (0)	17 (1)	0 (1)	6 (1)
F(2*B*#)	14 (1)	18 (2)	19 (1)	21 (3)	28 (3)	27 (3)

* Special positions.

The atoms of the asymmetric unit in the non-centrosymmetric model are shown in Figs. 1 and 2. In the centrosymmetric model the numbering of the atoms is analogous to the numbering shown on ring *A* in space group *R*3. The hydrogen atoms are numbered according to the carbon atoms to which they are attached.

Discussion of the centrosymmetric structure

The discussion of the structure is restricted to the centrosymmetric model for the following reason. The two structures show no significant differences. Moreover, averages of bond distances and angles related by a pseudo-centre in the non-centrosymmetric model are very close to the corresponding values in the centrosymmetric model.

Ring conformation

Bond distances, angles and the least-squares plane of the PyNO group are shown in Table 10. The dihedral angle between the aromatic rings is 0° (± 1°). Standard deviations are based on errors in both the cell constants and the complete covariance matrix of the last least-squares refinement cycle. The results are compared with literature data (Table 11, note the local C_2 symmetry assumed for the averaging of the bond distances). Contrary to earlier publications (Horrocks, Templeton & Zalkin, 1968; Sager, Williams & Watson, 1967; Tsoucaris, 1961) there is no indication of an out-of-plane position of the oxygen atom with respect to the aromatic ring.

Coordination of the nickel cation

The coordination of the Ni^{II} cation by the oxygen atoms is almost octahedral. The Ni–O–N angles are

Table 10. *Bond distances, angles and least-squares plane of the* PyNO *ring*

O—N	1·332 (1) Å	O—N—C(1)	120·2 (1)°
N—C(1)	1·333 (2)	O—N—C(5)	118·3 (1)
N—C(5)	1·349 (1)	C(1)-C(2)-C(3)	119·6 (2)
C(1)-C(2)	1·373 (3)	C(2)-C(3)-C(4)	118·5 (2)
C(2)-C(3)	1·384 (3)	C(3)-C(4)-C(5)	120·9 (2)
C(3)-C(4)	1·365 (4)	C(4)-C(5)-N	119·3 (2)
C(4)-C(5)	1·370 (1)	C(5)-N—C(1)	121·3 (1)
		N—C(1)-C(2)	120·4 (1)

C(1)-H(1)	1·00 (2)
C(2)-H(2)	0·93 (2)
C(3)-H(3)	0·89 (3)
C(4)-H(4)	1·05 (2)
C(5)-H(5)	0·95 (2)

Least-squares plane of nitrogen and the carbon atoms:

$$-0{\cdot}8782X-0{\cdot}4698Y+0{\cdot}0901Z+0{\cdot}8257=0\,.$$

Distances of atoms to the plane (Å)

N	0·007	O	−0·012
C(1)	−0·002	H(1)	0·119
C(2)	−0·003	II(2)	−0·046
C(3)	0·004	H(3)	−0·017
C(4)	0·001	H(4)	−0·009
C(5)	−0·006	H(5)	0·006

nearly 120°. The non-linear Ni–O–N arrangement lowers the symmetry of coordination by the PyNO molecules to S_6. Distances and angles are tabulated in Table 12. Fig. 3 shows the environment of the nickel cation.

The Ni–O distances are about the same as those found in $Ni(C_5H_5O_2)_2(PyNO)_2$ (2·046 Å, Horrocks *et al.*, 1968). The dihedral angle of the least-squares plane of the PyNO ring with the Ni–O–N plane is in agreement with the value of Kepert *et al.* (1973) for isomorphous $Hg(PyNO)_6(ClO_4)_2$. Similar values were found by Blom, Penfold & Robinson (1969) for other PyNO complexes.

Table 12. *Coordination of the* Ni *ion*

Single prime: rotation 120°
Double prime: rotation 120° + inversion

Distances (Å)		Angles (°)	
Ni—O	2·060 (1)	Ni—O -N	119·0 (1)
O-O′	2·920 (2)	O-Ni-O′	90·3 (1)
O-O″	2·906 (2)	O-Ni-O″	89·7 (1)
N-N′	3·924 (2)	N-Ni-N′	83·5 (1)
N-N″	4·395 (2)	N-Ni-N″	96·5 (1)

Angle Ni-O-N-PyNO-plane: 71·4°.

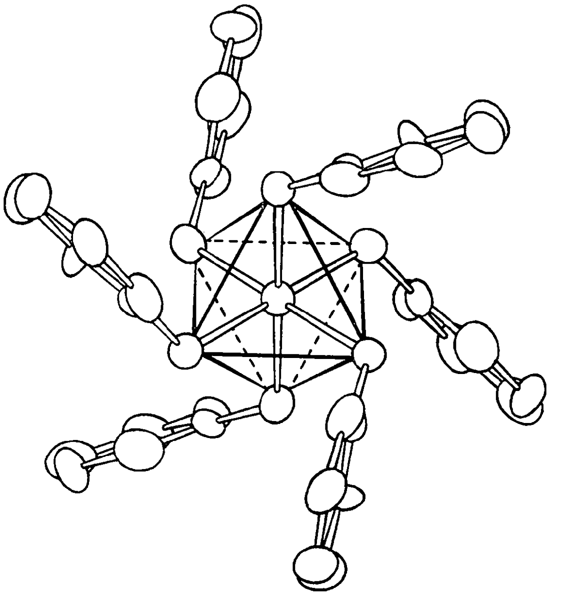

Fig. 3. Coordination of Ni by the PyNO rings, viewed along the C_3 axis. For clarity the oxygen octahedron is drawn.

Table 11. *Comparison of bond distances* (Å) *in* PyNO

Reference*	O-N	N-C(1)	N-C(5)	C(1)-C(2)	C(4)-C(5)	C(2)-C(3)	C(3)-C(4)
a	1·37	1·36	1·31	1·37	1·40	1·37	1·40
b	1·33 (2) 1·37 (2)	1·34 (2)† 1·34 (2)		1·37 (2) 1·38 (2)		1·35 (2) 1·39 (2)	
c	1·34 (1) 1·33 (1)	1·34 (1) 1·35 (2)	1·35 (1) 1·32 (1)	1·38 (2) 1·37 (2)	1·40 (2) 1·40 (2)	1·36 (1) 1·36 (2)	1·38 (2) 1·37 (2)
d	1·31 (1) 1·36 (1)	1·38 (1) 1·31 (1)	1·35 (1) 1·31 (2)	1·34 (2) 1·39 (2)	1·39 (2) 1·42 (2)	1·38 (1) 1·35 (2)	1·39 (1) 1·40 (1)
e	1·37 (2)	1·37 (2)	1·33 (2)	1·38 (3)	1·45 (3)	1·48 (3)	1·37 (3)
f	1·34 (1) 1·32 (1)	1·33 (1) 1·33 (1)	1·35 (1) 1·35 (1)	1·37 (1) 1·37 (2)	1·40 (1) 1·36 (2)	1·33 (1) 1·37 (2)	1·35 (1) 1·42 (2)
g	1·36 (1) 1·36 (1)	1·34 (1) 1·37 (1)	1·35 (1) 1·33 (1)	1·39 (1) 1·41 (1)	1·40 (1) 1·40 (1)	1·38 (1) 1·39 (1)	1·40 (1) 1·41 (1)
h	1·35 (2)	1·34 (2)	1·34 (2)	1·39 (3)	1·41 (3)	1·36 (3)	1·41 (3)
i	1·32 (3)	1·35 (4)	1·36 (3)	1·48 (4)	1·36 (4)	1·39 (5)	1·41 (5)
Averaged values	1·345	1·342		1·390		1·383	
This study	1·332 (1)	1·341 (1)		1·371 (2)		1·375 (3)	

**a* PyNO.HCl (Tsoucaris, 1961). *b* PyNO (Ülkü, Huddle & Morrow, 1971). *c* $Cu(PyNO)_4(ClO_4)_2$ (Lee, Brown & Melsom, 1969*a*). *d* $Cu(PyNO)_4(BF_4)_2$ (Lee, Brown & Melsom, 1969*b*). *e* $Sn(PyNO)_2(CH_3)_2Cl_2$ (Blom, Penfold & Robinson, 1969). *f* $Ni(PyNO)_2(C_5H_7O_2)_2$ (Horrocks, Templeton & Zalkin, 1968). *g* $Cu(PyNO)_2(NO_3)_2$ (Šćavničar & Matković, 1969). *h* $Cu_2(PyNO)_2Cl_4$ (Sager, Williams & Watson, 1967). *i* $Hg(PyNO)_6(ClO_4)_2$ (Kepert, Taylor & White, 1973).

†Molecules contain twofold axis.

The coordination of nickel by six PyNO ligands has been investigated by means of several physical techniques. A brief summary of those data, compared with our results, follows.

From n.m.r.-contact shifts Kluiber & Horrocks (1965) determined a Ni–O–N angle in the range 114–125° in solution.

From combined data of infrared and visible spectra, n.m.r. and magnetic moments Herlocker, Drago & Imhof Meek (1966), Whyman, Hatfield & Paschal (1967) and Reedijk (1969) conclude:

(i) The nickel is surrounded octahedrally by six oxygen atoms.

(ii) The anions do not take part in the coordination of the nickel ion.

However, the conclusion that the octahedron is distorted is controversial (Byers, Lever & Parish, 1968). Considering the almost perfect octahedral symmetry of the oxygen environment of Ni and in view of the decreasing influence of the other atoms on the crystal field of Ni ($\sim r^{-5}$), we may conclude that the interpretation of Reedijk is reliable within the accuracy of the method. Single crystal UVV and e.p.r. measurements will be made to compare the geometrical environment of Ni with the splitting of degenerate levels.

It is interesting to note that a successful interpretation of far-infrared spectra of the isomorphous coordination complexes could be made on the basis of an S_6 model (van Ingen Schenau *et al.*, 1974).

Anions

The geometry of the anions is reported in Table 13. In the centrosymmetric model we refined one parameter, α, for the occupancy ratio of the disordered BF_4^- groups. A final value of 76% was obtained, corresponding to 76% BF_4^- and (100–76)% $BF_4^-\#$.

A similar procedure was followed for the non-centrosymmetric model. We refined a parameter α for the ratio of BF_4^- (*A*) and BF_4^- (*A*#) and a parameter β for BF_4^- (*B*) *vs.* BF_4^- (*B*#). Final values were $\alpha=60$ and $\beta=75\%$, resulting in 60% BF_4^- (*A*), 40% BF_4^- (*A*#), 75% BF_4^- (*B*) and 25% BF_4^- (*B*#).

Table 13. *Geometry of the tetrafluoroborate anion*

Distances (Å)		Angles (°)	
B—F(1)	1·29	F(1)—B—F(2)	109
B—F(2)	1·36	F(2)—B—F(2)′	110
B#-F(1)#	1·22	F(1)#-B#-F(2)#	107
B#-F(2)#	1·28	F(2)#-B#-F(2)′#	112

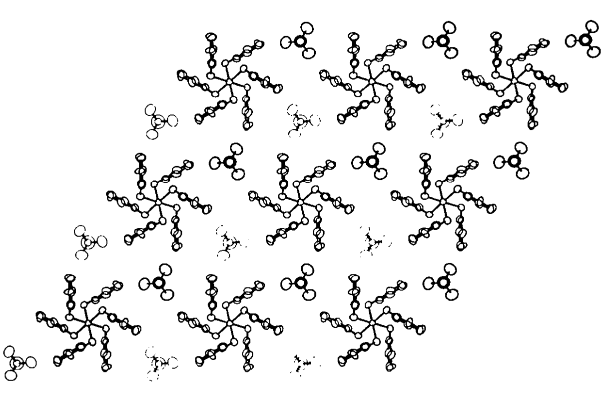

Fig. 4. Projection of nine molecular units along [001]. The relative height with respect to the plane (001) is indicated by the thickness of the circles.

Crystal structure

Short non-bonded distances between anions and cations are listed in Table 14. The shortest distance between two BF_4^- groups is observed for F(1)–F(1) (3·00 Å). This distance compares favourably with the oxygen–oxygen distance of 2·97 Å found by Kepert *et al.* (1973). Although this distance is rather short, it is longer than the van der Waals distance between fluorine atoms (2·66 Å, Shannon & Prewitt, 1969). The distances reported in Table 14 give no reason to assume hydrogen bonding between fluorine and carbon atoms [see Bondi (1964), Hamilton & Ibers (1968)]. This is also in agreement with the infrared spectra of BF_4^- (Reedijk, 1969), which show no significant distortion of the local T_d symmetry.

Table 14. *Short cation–anion, anion–anion and cation–cation distances*

	Operation on the second atom			
C(4)—F(1)#	x,	y,	z	3·39 Å
C(4)—F(2)	x,	y,	z	3·38
C(5)—F(1)#	x,	y,	z	3·06
F(2)#-C(2)	$x+y-\frac{1}{3}$,	$\bar{x}-\frac{2}{3}$,	$z-\frac{2}{3}$	3·41
F(2)#-C(3)	$\bar{x}-\frac{2}{3}$,	$\bar{y}+\frac{2}{3}$,	$\bar{z}+\frac{2}{3}$	3·27
F(1)—F(1)	x,	$\bar{y}$,	$\bar{z}$	3·00
C(4)—O	$\bar{x}+\frac{2}{3}$,	$\bar{y}+\frac{1}{3}$,	$\bar{z}+\frac{1}{3}$	3·45
C(4)—N	$\bar{x}+\frac{2}{3}$,	$\bar{y}+\frac{1}{3}$,	$\bar{z}+\frac{1}{3}$	3·38
C(5)—C(5)	$\bar{x}+\frac{2}{3}$,	$y+\frac{1}{3}$,	$\bar{z}+\frac{1}{3}$	3·38
F(1)#-H(5)	x,	y,	z	2·41
F(1)#-H(5)	$\bar{y}$,	$x-y$,	z	2·41
F(2)#-H(3)	$\bar{x}-\frac{2}{3}$,	$\bar{y}+\frac{2}{3}$,	$\bar{z}+\frac{2}{3}$	2·44
F(2)#-H(2)	$\bar{y}+\frac{2}{3}$,	$x-y+\frac{1}{3}$,	$z-\frac{2}{3}$	2·58

Fig. 4 shows one layer of the structure in a projection along [001]. The stacking of the $Ni(PyNO)_6$ groups is intermediate between simple cubic ($R\bar{3}$ with $\alpha=90°$) and close-packed cubic ($R\bar{3}$ with $\alpha=60°$). Since the angle of the rhombohedral cell (81·36°) is quite close to that of the ideal cubic cell (90°) we consider the structure to display a simple cubic packing. Kepert *et al.* (1973) designate the isomorphous structure of $Hg(PyNO)_6(ClO_4)_2$ as face-centered cubic.

The shortest Ni–Ni distances are 9·579 Å. Within a distance of 3·5 Å each $Ni(PyNO)_6$ group is surrounded by 8 BF_4^- groups. Within 3·5 Å the BF_4^- groups are enclosed by one neighbouring BF_4^- anion and four $(PyNO)_6$ cations.

Comparison of our results with those of Kepert *et al.* (1973) indicates that the geometries of our structure and $Hg(PyNO)_6(ClO_4)_2$ are roughly the same. It remains to been seen whether or not the anions of the Hg compound are also disordered. Owing to the small amount of photographic data (345 reflexions) combined with the dominant influence of the mercury atom on the scattering one cannot draw a definite conclusion.

Calculations

All calculations were performed on IBM 360/65 and 370/158 computers of the Central Computing Centre of the University of Leiden. For the multisolution method a program described by Motherwell & Isaacs (1971) was employed. Least-squares refinement was performed with the *ORFLS* program (Busing, Martin & Levy, 1962), modified by Rutten (Geise, Romers & Rutten, 1966). Computer drawings were made by *ORTEP* (Johnson, 1965) and geometrical computations partially by *ORFFE* (Busing, Martin & Levy, 1964). The remaining programs were developed in our laboratory.

The authors wish to express their appreciation to Dr J. Reedijk and Drs R. A. G. de Graaff for valuable discussions.

The investigation was supported by the Foundation for Investigations by means of X-ray and Electron Diffraction (FOMRE), with financial aid from the Netherlands Organization for the Advancement of Pure Research (ZWO).

References

Blom, E. A., Penfold, B. R. & Robinson, W. T. (1969). *J. Chem. Soc.* (*A*), pp. 913–917.

Bondi, A. (1964). *J. Phys. Chem.* **68**, 441–451.

Busing, W. R., Martin, K. O. & Levy, H. A. (1962). *ORFLS*. Report ORNL-TM-305, Oak Ridge National Laboratory, Oak Ridge, Tennessee.

Busing, W. R., Martin, K. O. & Levy, H. A. (1964). *ORFFE*. Report ORNL-TM-306, Oak Ridge National Laboratory, Oak Ridge, Tennessee.

Byers, W., Lever, A. B. P. & Parish, R. V. (1968). *Inorg. Chem.* **7**, 1835–1840.

Cromer, D. T. & Waber, J. T. (1965). *Acta Cryst.* **18**, 104–109.

Garvey, R. G., Nelson, J. H. & Ragsdale, R. O. (1968). *Coord. Chem. Rev.* **3**, 375–407.

Geise, H. J., Romers, C. & Rutten, E. (1966). *Acta Cryst.* **20**, 249–263.

Germain, G. & Woolfson, M. M. (1968). *Acta Cryst.* B**24**, 91–96.

Gomes de Mesquita, A. H. (1962). Thesis, Amsterdam.

Graaff, R. A. G. de (1973). *Acta Cryst.* A**29**, 298–301.

Gramaccioli, C. A. & Zechmeister, K. (1972). *Acta Cryst.* A**28**, 154–158.

Hamilton, W. C. (1964). *Statistics in Physical Science*. New York: Ronald Press.

Hamilton, W. C. & Ibers, J. A. (1968). *Hydrogen Bonding in Solids*. New York: Benjamin.

Herlocker, D. W., Drago, R. S. & Imhof Meek, V. (1966). *Inorg. Chem.* **5**, 2009–2015.

Horrocks, W. D., Templeton, D. H. & Zalkin, A. (1968). *Inorg. Chem.* **7**, 1552–1557.

Ingen Schenau, A. D. van, Reedijk, J. & Groeneveld, W. L. (1974). *Spectrochim. Acta*, **30**A 213–221.

International Tables for X-ray Crystallography (1962). Vol. III. Birmingham: Kynoch Press.

Joesten, M. D., Hussain, M. S. & Lenhert, P. G. (1970). *Inorg. Chem.* **9**, 151–161.

Johnson, C. K. (1965). *ORTEP*. Report ORNL-3794, Oak Ridge National Laboratory, Oak Ridge, Tennessee.

Kakiuti, Y., Kida, S. & Quagliano, J. V. (1963). *Spectrochim. Acta*, **19**, 201–211.

Karayannis, N. M., Pytlewski, L. L. & Mikulski, C. M. (1973). *Coord. Chem. Rev.* **11**, 93–159.

Karle, J. (1968). *Acta Cryst.* B**24**, 182–186.

Karle, J. & Hauptman, H. (1956). *Acta Cryst.* **9**, 635–651.

Kepert, D. L., Taylor, D. & White, A. H. (1973). *J. Chem. Soc. Dalton*, pp. 670–673.

Kluiber, R. W. & Horrocks, W. D. (1965). *J. Amer. Chem. Soc.* **87**, 5350–5356.

Lee, J. D., Brown, D. S. & Melsom, B. G. A. (1969*a*). *Acta Cryst.* B**25**, 1378–1385.

Lee, J. D., Brown, D. S. & Melsom, B. G. A. (1969*b*). *Acta Cryst.* B**25**, 1595–1601.

Leeuwen, P. W. N. M. van & Groeneveld, W. L. (1967). *Inorg. Nucl. Chem. Lett.* **3**, 145–146.

Motherwell, W. D. S. & Isaacs, N. W. (1971). *Acta Cryst.* A**27**, 681–682.

Pappas, A. J., Osterman, F. A. & Powell, H. B. (1970). *Inorg. Chem.* **9**, 2695–2698.

Reedijk, J. (1969). *Rec. Trav. Chim. Pays-Bas*, **88**, 499–512.

Sager, R. S., Williams, R. J. & Watson, W. H. (1967). *Inorg. Chem.* **6**, 951–955.

Šćavničar, S. & Matković, B. (1969). *Acta Cryst.* B**25**, 2046–2055.

Schenk, H. (1972). *Acta Cryst* A**28**, 412–422.

Shannon, R. D. & Prewitt, C. T. (1969). *Acta Cryst.* B**25**, 925–946.

Tsoucaris, G. (1961). *Acta Cryst.* **14**, 914–917.

Ülkü, D., Huddle, B P. & Morrow, J. C. (1971). *Acta Cryst.* B**27**, 432–436.

Whyman, P., Hatfield, W. E. & Paschal, J. S. (1967). *Inorg. Chim. Acta*, **1**, 113–119.